Kinetics of the Gas-Phase Reactions of OH and NO_3 Radicals and O_3 with Allyl Alcohol and Allyl Isocyanate

James K. Parker*,† and Cyntia Espada-Jallad

Midwest Research Institute, 425 Volker Boulevard, Kansas City, Missouri 64110

Received: June 15, 2009; Revised Manuscript Received: July 29, 2009

Rate constants for the gas-phase reactions of OH radical, NO_3 radical, and ozone with allyl alcohol (AAL) and allyl isocyanate (AIC) have been measured using relative rate methods at atmospheric pressure in purified air. The experimental Arrhenius expression obtained for the reaction of the OH radical with AAL is $(1.68 \pm 0.89) \times 10^{-12} \times \exp(1100/T)$ cm^3 molecule^{-1} s^{-1}, for $T = 282-315$ K; the Arrhenius expression for the reaction of OH radical with AIC is $(1.94 \pm 1.04) \times 10^{-14} \times \exp(2207/T)$ cm^3 molecule^{-1} s^{-1}, for $T = 282-317$ K, where the indicated errors are one least-squares standard deviation. All OH radical reaction rate constants have been measured relative to k(OH + α-pinene) and k(OH + 1,3,5-trimethylbenzene). The rate constant for the gas-phase reaction of OH radical with allyl alcohol-d_6 isotopomer (AAL-d_6) has been measured at $T = 298$ K, and the value is 5.10×10^{-11} cm^3 molecule^{-1} s^{-1}. The kinetic isotope effect is small, with k(AAL)/k(AAL-d_6) = 1.32. Rate constants for the gas-phase reactions of NO_3 radical with AAL [relative to k(NO_3 +methacrolein)] and O_3 [relative to k(O_3 + β-pinene)] have been measured, and the values are 7.7×10^{-15} cm^3 molecule^{-1} s^{-1} at $T = 298$ K and 1.6×10^{-17} cm^3 molecule^{-1} s^{-1} at $T = 296$ K, respectively. Rate constants for the gas-phase reactions of NO_3 radical and O_3 with AIC have been measured, and the values are 9.4×10^{-16} cm^3 molecule^{-1} s^{-1} at $T = 299$ K and 5.54×10^{-18} cm^3 molecule^{-1} s^{-1} at $T = 299$ K, respectively. Multireference ab initio calculations at the MRMP2/6-311G(d,p) level have been carried out for reactions of OH radical with AAL and AIC. Results indicate that prereactive hydrogen bonded complexes form in the entrance channels for these reactions.

Introduction

Unsaturated volatile organic compounds (VOCs) are emitted into the atmosphere from natural and anthropogenic sources.[1] These compounds undergo oxidative reactions with OH and NO_3 radicals and ozone. In particular, there is increasing interest in the atmospheric chemistry of oxygenated, unsaturated VOCs because these are thought to play a significant role in secondary organic aerosol formation.[2−5] In addition, some of the oxygenated VOCs are toxic, and so there is interest in how these anthropogenic compounds are transformed in the atmosphere. There is also interest in the mechanisms of reactions of OH radicals with hydrocarbons and oxygenated hydrocarbons. In a review of the formation of radical-molecule complexes,[6] Hansen and Francisco highlight the importance of the formation of prereaction hydrogen bonded complexes of the OH radical with small alkenes and acetone.

Previously, we reported results of relative rate experiments and ab initio calculations for reaction of the OH radical with isopropyl isocyanate [$(CH_3)_2$CHNCO; IIC] in the $T = 287-321$ K range.[7] IIC is a saturated, oxygenated VOC used in the plastics and pesticides industries and is very toxic on inhalation and skin exposure. The experimentally measured rate constant for this reaction showed a slight negative temperature dependence. Multilevel ab initio calculations confirmed that the reaction mechanism involves formation of hydrogen bonded complexes of OH and IIC in the reaction entrance channels, followed by rearrangement through a submerged first-order saddle point to form products prop-2-yl isocyanate radical and water. That formation of hydrogen bonded prereaction complexes can lower the energy of this transition state into the subthreshold regime demonstrates the important effect that the complex has on the reaction's energetics and resulting dynamics. Here, we extend the work to include experimental rate constant studies and ab initio calculations for the reactions of OH radicals with the unsaturated VOCs allyl isocyanate (CH_2═$CHCH_2NCO$; AIC) and allyl alcohol (CH_2═$CHCH_2OH$; AAL). This work is the first report in the literature of the rate constant for reaction of the OH radical with AIC and the first report of the temperature dependence of the reaction of the OH radical with AAL. In addition, we report for the first time the rate constants for reactions of the NO_3 radical and O_3 with AIC. We also present additional data for reactions of NO_3 radicals and O_3 with AAL. The results of the ab initio calculations indicate that OH radicals form hydrogen bonded prereaction complexes with the unsaturated, oxygenated VOCs AIC and AAL and that these complexes play a significant role in the resulting reaction dynamics.

Experimental Methods

Relative Rate Measurements. Rate constants for reactions of OH radicals were measured in a static reactor using a relative rate technique at atmospheric pressure in purified air.[4] α-Pinene and 1,3,5-trimethylbenzene were selected as the reference compounds because their rate constants for reaction with the hydroxyl radical are well-known and are similar in magnitude to that of AAL and AIC. The experimental method and apparatus have been described recently and will be briefly recounted here.[7] The reaction chamber consisted of a FEP-Teflon collapsible bag of 0.13 mm thickness and 220 L in volume

* Corresponding author. Phone: 919-549-4293. E-mail: james.kenneth.parker@arl.army.mil.

† Present address: U.S. Army Research Office, 4300 S. Miami Blvd., Durham, NC 27703.

10.1021/jp9055939 CCC: $40.75
Published on Web 08/17/2009

surrounded by 16 40-W fluorescent black lamps with $\lambda_{max} =$ 350 nm (Sylvania F40/350 BL). The Teflon reactor and associated lighting was placed in a completely dark cabinet to exclude unwanted light. Temperature control was achieved by a flow of 1.7 m^3 min^{-1} thermostatted air through the insulated cabinet and around the outside of the collapsible Teflon reaction chamber. Temperatures were recorded at positions just above and below the reactor with calibrated T-type thermocouples. The experimental uncertainty in temperature is ± 1 K.

Reactants were introduced into the chamber by injection into a stream of purified air (Aadco zero air generator, model 737) at a flow rate of 8 standard L/ min. Neat liquid allyl alcohol (Sigma-Aldrich, ≥99%), neat liquid allyl alcohol-d_6 (Isotec, 99.9% pure, 99 atom % D), neat liquid allyl isocyanate (Sigma-Aldrich, 98%), α-pinene (Sigma-Aldrich, 99%), β-pinene (Sigma-Aldrich, 98%), methacrolein (Sigma-Aldrich, 95%), methyl nitrite (Midwest Research Institute, 99.5+%), and 2 cm^3 of nitric oxide (Linde, 99.5%) diluted to 10 cm^3 with nitrogen (Nitrogen Air Pressure Co., 99.999%) to suppress its oxidation upon introduction into the air stream were injected into the flow of purified air into a 1/4-in. i.d. silco-coated steel line (Restek) via a tee capped at the middle port with a septum. The initial gas-phase concentrations (molecules cm^{-3}) of the reactants were $[AAL]_0 \approx 1.2 \times 10^{13}$, $[AIC]_0 \approx 1.2 \times 10^{13}$, [α-pinene or β-pinene]$_0 \approx 7.2 \times 10^{12}$, [1,3,5-trimethylbenzene]$_0 \approx 3.6 \times 10^{12}$, [methacrolein]$_0 \approx 3.6 \times 10^{12}$, $[NO]_0 \approx 2.4 \times 10^{14}$, and $[CH_3ONO]_0 \approx 2.4 \times 10^{14}$.

Hydroxyl radicals were generated by the UV photolysis of methyl nitrite in air. To minimize temperature variations in the chamber, during irradiations, only eight of the lamps were turned on. The OH radical reactions were carried out in excess nitric oxide to suppress formation of ozone. The concentrations of NO and NO_2 were measured periodically with a chemiluminescence analyzer (Thermo Electron, model 42*i*). The initially measured NO concentration (after the mixtures were prepared but before any photolysis) was found to be approximately 1×10^{14} molecules cm^{-3} after preparation of the mixtures. It was observed that ~60% of the NO was oxidized upon introduction of the 20% NO/80% N_2 mixture into the flow of purified air.

Nitrate radicals were generated by the thermal decomposition of N_2O_5 in air. N_2O_5 was prepared from the gas-phase reaction of ozone with nitrogen dioxide. The synthesis was carried out by titration of a flow of NO_2 with O_3 through glass lines until the color of the gas mixture changed from brown to colorless. A significant amount of heat was generated in this reaction. The gas flow passed over P_2O_5 drying agent, and then N_2O_5 condensed in a trap held at dry ice/acetone temperature.

N_2O_5 was added to the reaction chamber by allowing the vapors from the solid sample to expand into an evacuated 125 cm^3 glass vessel. The vessel is cylindrically shaped with an input tube at one end of the cylinder axis and an output tube on the opposite end. The vessel was filled with approximately 3 Torr of N_2O_5 vapor. The pressure in the vessel was measured by calibrated baratrons. Upon filling of the vessel with N_2O_5 vapor, purified air was added to the vessel until the total pressure reached 760 Torr, then the contents of the vessel was pushed into the reaction chamber by a flow of zero air at 250 sccm for 2.5 min. A fan in the bottom of the reaction chamber rapidly mixed the contents while the N_2O_5 vapors entered.

Ozone was made by passing an electric discharge through pure oxygen gas, which was contained in a glass U-tube. The bottom of the U-tube was submerged in liquid nitrogen so that the ozone condensed to the solid state as it formed. Residual oxygen was then pumped off the solid ozone. The ozone was then allowed to sublime, and its vapors filled the 125 cm^3 sample bulb to approximately 1 Torr pressure at 20 °C. The sample bulb was then filled with zero air to 760 Torr pressure, and the contents of the bulb was flushed into the 220-L Teflon reactor containing the target compound−reference compound−OH scavenger−air mixture. In AAL experiments, acetaldehyde was present at 5.4×10^{15} molecules cm^{-3} as an OH scavenger. In the AIC experiment, acetaldehyde was present at 3.5×10^{15} molecules cm^{-3} as an OH scavenger. The concentration of acetaldehyde used was such that 99+% of OH radicals present in the chamber (due to secondary chemistry of the ozone/alkene reactions) would be absorbed by acetaldehyde. As the ozone/air mixture entered the reactor, a fan in the bottom of the reactor rapidly mixed the contents. The nominal initial concentration of ozone in these experiments is 2.4×10^{13} molecules cm^{-3}. The concentration of ozone was monitored by absorption of 254 nm light by the gas mixture in a photocell (UV-106 Ozone Analyzer, Ozone Solutions, Sioux City, Iowa).

The change in concentration of target and reference compounds was followed by gas chromatography (Hewlett-Packard, G1530A) with electron-ionization mass spectrometric detection (Agilent, 5975 MSD) at $m/z = 57$ for AAL, $m/z = 56$ for AIC, $m/z = 91$ for toluene, $m/z = 105$ for 1,3,5-trimethylbenzene, and $m/z = 93$ for α- and β-pinene. For the analyses, gas samples of 100 cm^3 volume were collected from the reaction chamber with the aid of a mass flow meter and digital stopwatch onto Tenax-TA solid adsorbent. Target and reference compounds were desorbed from the adsorbent in a two-stage method. The first stage of the thermal desorption heats the adsorbent to 240 °C at a helium carrier gas flow of 20 standard cm^{-3} min^{-1} and deposits the analytes onto a Tenax-TA cold trap held at 0 °C. In the focusing stage, the cold trap is flash-heated to 240 °C (in about 3 s) under a flow of He, and the analytes are deposited onto a RTx-1701 fused-silica microcapillary column (Restek, model Rtx-5MS, 15 m × 0.25 mm, 1 μm) held at 40 °C for 1.0 min and temperature-programmed to 175 at 15 °C min^{-1}. Analytical uncertainties were estimated from replicate analyses in the dark and were typically 3−5% for target and reference compounds.

Rate constants for the reactions of OH, NO_3, and O_3 with AAL and AIC were measured using relative rate techniques in which the concentrations of AAL and AIC and reference compounds (whose OH, NO_3, and O_3 reaction rate constants are reliably known) were measured in the presence of the OH radical, theNO_3 radical, and O_3. The chemical reactions which consume the target and reference compounds are given in eqs 1 and 2.

$$\left\{\begin{matrix}\mathrm{OH}\\ \mathrm{NO_3}\\ \mathrm{O_3}\end{matrix}\right\} + \text{target compound} \rightarrow \text{products} \qquad (1)$$

$$\left\{\begin{matrix}\mathrm{OH}\\ \mathrm{NO_3}\\ \mathrm{O_3}\end{matrix}\right\} + \text{reference compound} \rightarrow \text{products} \qquad (2)$$

When the target and reference compounds are lost solely to reaction with OH, NO_3, or O_3, then,

$$\ln\left\{\frac{[\text{target}]_0}{[\text{target}]_t}\right\} - D_t = \frac{k_1}{k_2}\left[\ln\left\{\frac{[\text{reference}]_0}{[\text{reference}]_t}\right\} - D_t\right] \qquad (3)$$

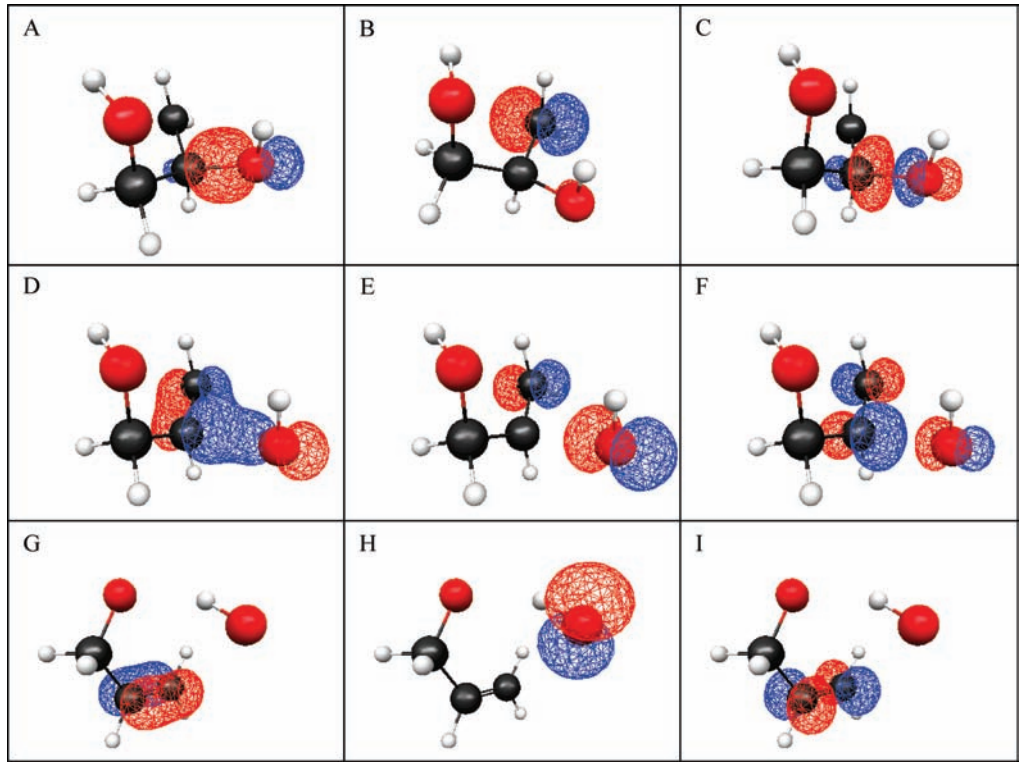

Figure 1. MCSCF natural orbitals of the three-electron, three-orbital active space for addition of OH radical to the secondary carbon atom of AAL. (A−C) Propan-3-yl-1,2-diol with a C−O equilibrium distance of 1.44 Å; (D−F) first-order saddle point connecting OH radical and AAL reactants to propan-3-yl-1,2-diol product with an equilibrium C−O distance of 2.01 Å; (G−I) hydrogen bonded complex of OH and AAL in the reactant entrance channel, which precedes formation of propan-3-yl-1,2-diol with an equilibrium C−O distance of 3.4 Å.

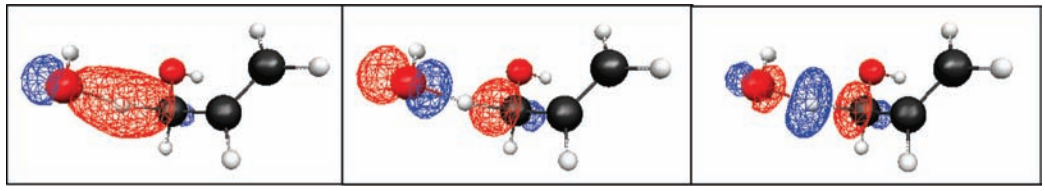

Figure 2. MCSCF natural orbitals (at the saddle point) used in the three-electron, three-orbital active space for transfer of a hydrogen atom from the CH_2 moiety of AAL to the OH radical.

In eq 3, $[\text{target}]_0$ and $[\text{reference}]_0$ are the concentrations of AAL or AIC and reference compound, respectively, at time zero (prior to any chemical reaction); $[\text{target}]_t$ and $[\text{reference}]_t$ are the corresponding concentrations at time t; D_t is a factor to account for dilution due to addition of ozone/air or N_2O_5/air mixtures to the chamber during experiments ($D_t = 0$ for the OH radical reactions and $D_t = 0.0035$ per N_2O_5 or O_3 addition); and k_1 and k_2 are the rate constants for reactions 1 and 2, respectively.

Quantum Mechanical Calculations. Quantum mechanical calculations were carried out for the two combination channels and one hydrogen atom transfer channel in the reactions of OH radical with AAL and AIC using the software program GAMESS.[8] Reactions of NO_3 and O_3 have not been studied by QM calculations. Geometry optimizations to local minima and first-order saddle points were obtained with multiconfiguration self-consistent field theory[9] using three electrons in three active orbitals and the 6-311G(d,p) basis set.[10−25] This level of theory is abbreviated as (3,3)-MCSCF. The three electrons chosen for the active space in the two combination channels are the two electrons from the π-bond of AAL or AIC and the single radical electron of the OH radical. At long distances, the three orbtials used in the active space were the π-bonding orbital of AAL, the orbital containing the radical electron of the OH radical, and the π-antibonding orbital of AAL. At short distances, the three orbtials of the active space are the σ-bonding orbital of the newly formed C−O bond, the p atomic orbital of carbon containing the single electron of the propanyldiol radical product, and the σ-antibonding orbital of the newly formed C−O bond. The transition state region, with the C−O distance extending from about 1.8 to 2.2 Å, is characterized as intermediate between the long- and short-range conditions. Figure 1 presents these active space natural MCSCF orbitals for the reaction channel that forms propan-3-yl-1,2-diol radical from a combination of the OH radical with AAL. Analogous orbitals were chosen for the active space in the reaction channel that forms the propanyl-1,3-diol radical by a combination of OH and AAL. An analogous active space was chosen for the addition channels of the OH + AIC reaction (not shown).

MCSCF calculations were also carried out on the reaction channels where the OH radical attacks the CH_2 group of AAL (or AIC) to form the products water and prop-2-en-1-hydroxy-1-yl radical (prop-2-en-1-isocyano-1-yl radical). The three fully optimized natural MCSCF orbitals of the active space at the saddle point for the OH + AAL reaction are shown in Figure 2. A similar active space was chosen for the hydrogen atom transfer channel of the OH + AIC reaction (not shown). For all reaction channels, dynamical correlation energy was recovered from single-point energy calculations

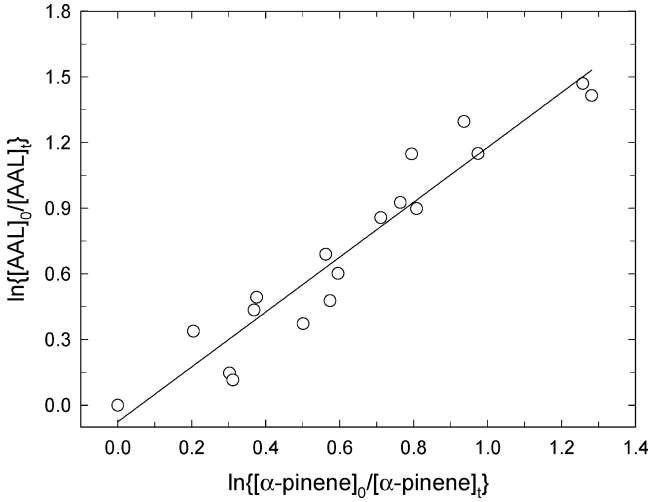

Figure 3. Plot of the data according to eq 3 for reaction of OH radical with allyl alcohol at $T = 300$ K with α-pinene as the reference compound.

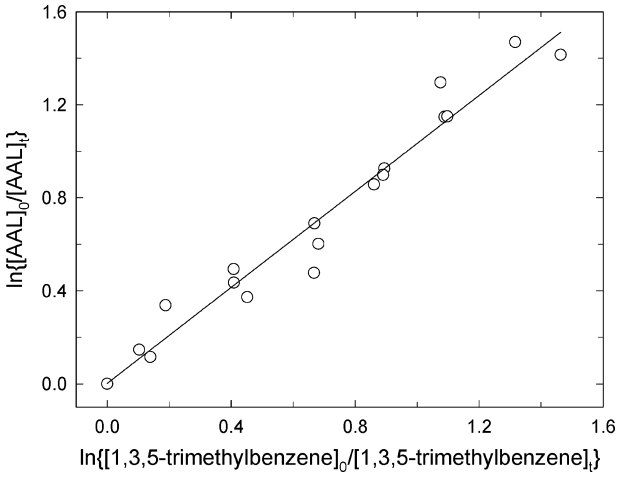

Figure 4. Plot of the data according to eq 3 for reaction of OH radical with allyl alcohol at $T = 300$ K with 1,3,5-trimethylbenzene as the reference compound.

via multiconfiguration second-order perturbation theory using the 6-311G(d,p) basis set. This level of theory is abbreviated as MRMP2/6-311G(d,p).[26,27]

Results

Photolysis and Dark Reactions. When purified air mixtures containing AAL or AIC and α-pinene and 1,3,5-trimethylbenzene (as reference compounds) were subjected to radiation from eight lamps for 20 min, no losses for any compound were observed. Hydroxyl radical experiments used the same light intensity for a total of 2 min duration. No significant dark losses (<5%) were observed when separate AAL/α-pinene/1,3,5-trimethylbenzene/air and AIC/α-pinene/1,3,5-trimethylbenzene/air mixtures were allowed to stand undisturbed for a 4 h period. All kinetics experiments were completed within a 4 h period from the time concentration monitoring began. These data show that dark decay and photolysis of AAL and AIC were of no importance in the irradiated CH_3ONO/NO/AAL/α-pinene/1,3,5-trimethylbenzene/air and CH_3ONO/NO/AIC/α-pinene/1,3,5-trimethylbenzene/air mixtures used to determine the OH radical rate constants. Dark loss was also of no importance in the NO_3 and O_3 rate constant experiments.

Rate Constants for Reactions with OH Radicals. CH_3ONO/NO/AAL/α-pinene/1,3,5-trimethylbenzene/air irradiations were

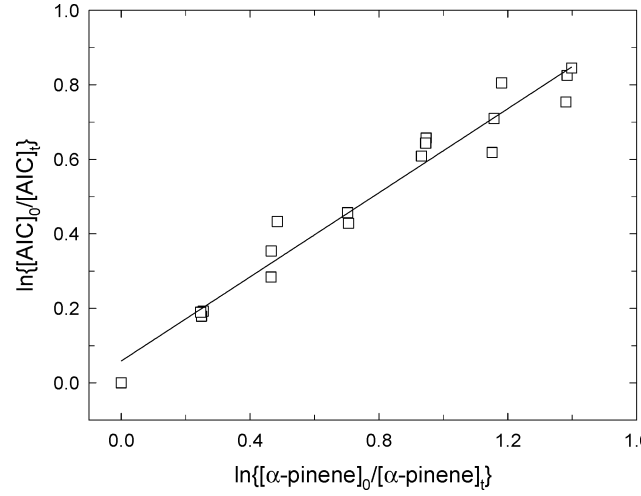

Figure 5. Plot of the data according to eq 3 for reaction of OH radical with allyl isocyanate at $T = 299$ K with α-pinene as the reference compound.

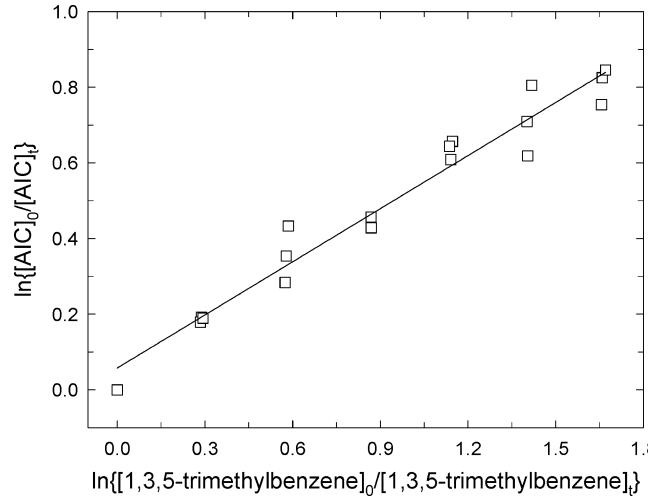

Figure 6. Plot of the data according to eq 3 for reaction of OH radical with allyl isocyanate at $T = 299$ K with 1,3,5-trimethylbenzene as the reference compound.

carried out in the $T = 282-315$ K range. CH_3ONO/NO/AIC/α-pinene/1,3,5-trimethylbenzene/air irradiations were carried out in the $T = 282-317$ K range. Representative data from the experiments are plotted in accordance with eq 3 in Figures 3−6. The resulting rate constant ratios, k_1/k_2, from the slopes of the linear-least-squares regressions are given in Table 1. Absolute values for k_1 are obtained by use of recommended rate constants of $k_2 = 1.21 \times 10^{-11} \times \exp(436/T)$ cm^3 molecule^{-1} s^{-1} for the reaction of OH radical with α-pinene[28] and $k_2 = 6.3 \times 10^{-12} \times \exp(670/T)$ cm^3 molecule^{-1} s^{-1} for the reaction of OH radical with 1,3,5-trimethylbenzene.[29] We note that a recent study[41] finds the temperature-dependent expression for $k_2 = 4.4 \times 10^{-12} \times \exp(738/T)$ cm^3 molecule^{-1} s^{-1} for reaction of OH with 1,3,5-trimethylbenzene. The resulting values for k_1 are listed in Table 1, with the indicated errors equal to 1 standard deviation. The data of Table 1 are plotted in Arrhenius form in Figure 7. The resulting Arrhenius expressions are $k(\mathrm{OH} + \mathrm{AAL}) = 1.68 \times 10^{-12} \times \exp[(1100 \pm 157)/T]$ cm^3 molecule^{-1} s^{-1} for $T = 282-315$ K, and $k(\mathrm{OH} + \mathrm{AIC}) = 1.94 \times 10^{-14} \times \exp[(2207 \pm 158)/T]$ cm^3 molecule^{-1} s^{-1} for $T = 282-317$ K.

Rate Constants for Reactions of AAL and AIC with NO_3. The reactions of NO_3 with AAL, AAL-d_6 (fully deuterated allyl alcohol), and AIC were carried out near ambient room temper-

TABLE 1: Rate Constant Ratios k_1/k_2 and Rate Constants k_1 (cm^3 molecule^{-1} s^{-1}) for the Reactions of the OH Radical with Allyl Alcohol, Allyl Alcohol-d_6, and Allyl Isocyanate with α-Pinene and 1,3,5-Trimethylbenzene as the Reference Compounds

T (K)	k_1/k_2	$10^{11} \times k_1$	ref compd
	AAL		
282	1.42 ± 0.08	8.02 ± 0.46	α-pinene
282	1.21 ± 0.06	8.20 ± 0.41	TMB
293	1.44 ± 0.05	7.71 ± 0.28	α-pinene
300	1.04 ± 0.12	6.13 ± 0.69	TMB
300	1.31 ± 0.18	6.77 ± 0.94	α-pinene
307	1.09 ± 0.08	6.10 ± 0.44	TMB
307	1.30 ± 0.07	6.48 ± 0.35	α-pinene
315	1.07 ± 0.05	5.63 ± 0.28	TMB
315	1.16 ± 0.05	4.82 ± 0.20	α-pinene
	AAL-d_6		
298	0.978 ± 0.045	5.11 ± 0.24	α-pinene
298	0.855 ± 0.038	5.10 ± 0.23	TMB
	AIC		
282	0.724 ± 0.044	4.90 ± 0.30	TMB
282	0.876 ± 0.054	4.97 ± 0.31	α-pinene
290	0.615 ± 0.056	3.89 ± 0.35	TMB
290	0.736 ± 0.059	4.00 ± 0.32	α-pinene
299	0.468 ± 0.025	2.78 ± 0.15	TMB
299	0.564 ± 0.029	2.94 ± 0.16	α-pinene
306	0.413 ± 0.012	2.33 ± 0.07	TMB
306	0.466 ± 0.013	2.35 ± 0.07	α-pinene
316	0.469 ± 0.020	2.47 ± 0.11	TMB
316	0.494 ± 0.018	2.38 ± 0.09	α-pinene
317	0.410 ± 0.017	2.14 ± 0.09	TMB
317	0.473 ± 0.02	2.26 ± 0.10	α-pinene

ature. Four to five additions of N_2O_5/air mixtures were added to the chamber during each experiment over a 4 h period. The amount of N_2O_5 added to the chamber was equivalent to ~6 × 10^{13} molecules cm^{-3} per addition, with D_t equal to 0.0035. Thermal decomposition of the N_2O_5 yielded the NO_3 radicals.[30,31] Methacrolein was used as the reference compound. A relative rate plot is shown for the reactions of NO_3 with AAL and AIC in Figure 8. Absolute values for k_1 are obtained by use of the

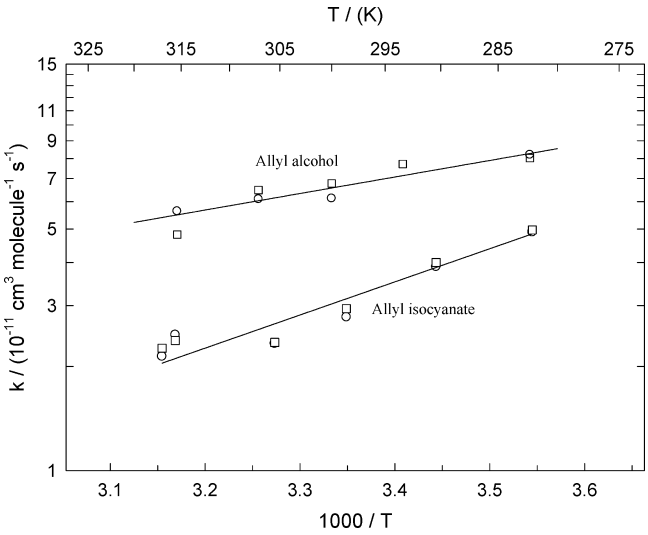

Figure 7. Arrhenius plots of the rate constants, k_1, for the reactions of OH radicals with allyl alcohol and allyl isocyanate. ○, relative to 1,3,5-trimethylbenzene; □, relative to α-pinene. The solid lines are linear regressions of the experimental data. k_1(OH + AAL) = 1.68 × 10^{-12} × exp[(1100 ± 157)/T] cm^3 molecule^{-1} s^{-1} and k_1(OH + AIC) = 1.94 × 10^{-14} × exp[(2207 ± 158)/T] cm^3 molecule^{-1} s^{-1}.

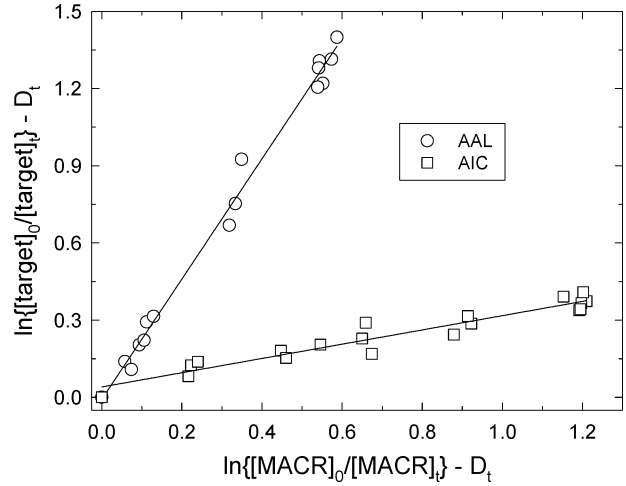

Figure 8. Plot of the data according to eq 3 for reaction of NO_3 radical with allyl alcohol at T = 298 K and allyl isocyanate at T = 299 K with methacrolein as the reference compound.

TABLE 2: Rate Constant Ratios k_1/k_2 and Rate Constants k_1 (cm^3 molecule^{-1} s^{-1}) for the Reactions of NO_3 Radical with Allyl Alcohol, Allyl Alcohol-d_6, and Allyl Isocyanate with Methacrolein as the Reference Compound

T (K)	k_1/k_2	$10^{15} \times k_1$	target compd
298	2.34 ± 0.06	7.7 ± 0.2	AAL
298	2.22 ± 0.04	7.6 ± 0.2	AAL-d_6
299	0.277 ± 0.019	0.94 ± 0.06	AIC

recommended rate constant of 3.4 × 10^{-15} cm^3 molecule^{-1} s^{-1} for k_2.[28] The resulting rate constants are given in Table 2, where the indicated errors are 1 least-squares standard deviation.

Rate Constants for Reactions of AAL and AIC with O_3. The reactions of O_3 with AAL, AAL-d_6, and AIC were carried out near ambient room temperature. One addition of an O_3/air mixture was added to the chamber per experiment. The amount of O_3 added was equivalent to ~2.4 × 10^{13} molecules cm^{-3}, with D_t equal to 0.0035. β-Pinene was used as the reference compound. A relative rate plot is shown for the reactions of O_3 with AAL and AIC in Figure 9. Absolute values for k_1 are obtained by use of the recommended rate constant 1.2 × 10^{-15} × exp(−1300/T) cm^3 molecule^{-1} s^{-1} for k_2.[28] The resulting rate

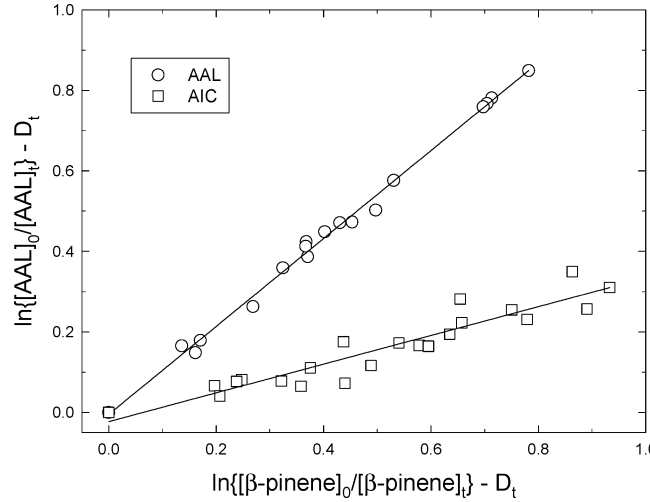

Figure 9. Plot of the data according to eq 3 for reaction of O_3 with allyl alcohol at T = 296 K and allyl isocyanate at T = 299 K with β-pinene as the reference compound.

constants are given in Table 3, where the indicated errors are 1 least-squares standard deviation.

Ab Initio Potential Energies for Reactions of OH Radical with AAL and AIC. Potential energy scans were conducted for addition of the OH radical to AAL to form propan-3-yl-1,2-diol (reaction channel 4a) and propan-2-yl-1,3-diol (channel 4b), and for transfer of a hydrogen atom from the CH_2 moiety of AAL to the OH radical (channel 4c). The reaction channels are

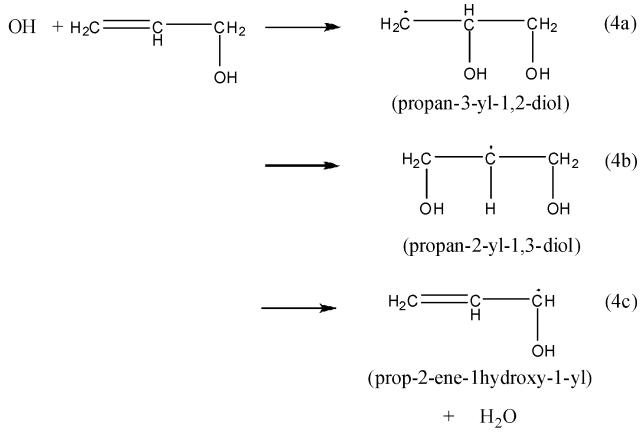

For channels 4a and b, the potential energy scans were carried out at the (3,3)-MCSCF/6-311G(d,p) level of theory by holding the C−O distance fixed and optimizing the remaining degrees of freedom. The C−O distance is defined as the distance from one of the unsaturated carbon atoms of AAL to the oxygen atom of the OH radical. This approach allowed for easy identification of the single saddle point on reaction channels 4a and b. Dynamical correlation energy was recovered via single-point multireference MP2 calculations at each optimized MC-SCF structure. The resulting MRMP2/6-311G(d,p) potential energy scans are shown in Figures 10 and 11. Structural renditions of the stationary points involved in both addition channels are shown in Figure 12. Table 4 lists the relative energies of the stationary points involved in reaction channels 4a−c.

Potential energy scans were conducted for addition of the OH radical to AIC to form propan-3-yl-1-isocyano-2-ol product (reaction channel 5a) and propan-2-yl-1-isocyano-3-ol (channel 5b) and for transfer of a hydrogen atom from the CH_2 moiety of AIC to the OH radical (channel 5c). The reaction channels are

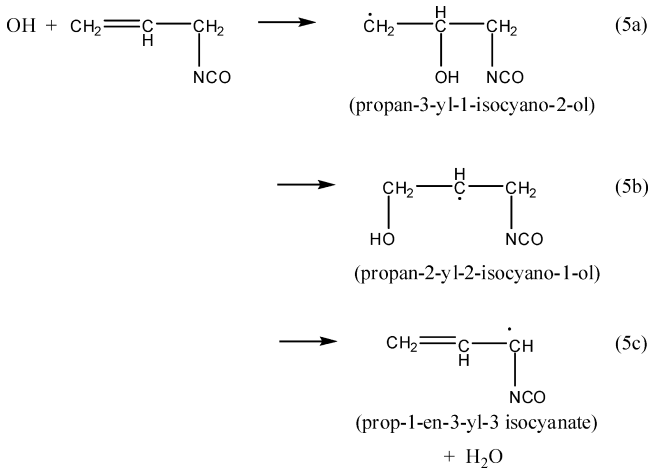

TABLE 3: Rate Constant Ratios k_1/k_2 and Rate Constants k_1 (cm^3 $molecule^{-1}$ s^{-1}) for the Reactions of O_3 with Allyl Alcohol, Allyl Alcohol-d_6, and Allyl Isocyanate with β-Pinene as the Reference Compound

T (K)	k_1/k_2	$10^{18} \times k_1$	target compd
296	1.09 ± 0.02	16.3 ± 0.3	AAL
298	1.21 ± 0.02	18.4 ± 0.3	AAL-d_6
299	0.357 ± 0.029	5.54 ± 0.45	AIC

Discussion

This work reports the temperature dependence of the rate constant for the OH + AAL reaction. From the Arrhenius expression, the value of k(OH + AAL) is (6.74 ± 1.35) × 10^{-11} cm^3 $molecule^{-1}$ s^{-1} at T = 298 K, with an overall estimated uncertainty of 20%. The rate constant for reaction of OH radical with allyl alcohol has been reported by several research groups. All of these previous studies, except two, have been near T = 298 K: Papagni et al. report a value of k(OH + AAL) = (5.46 ± 0.35) × 10^{-11} cm^3 $molecule^{-1}$ s^{-1} at T = 296 ± 2 K at atmospheric pressure in purified air using a relative rate method with 1,3,5-trimethylbenzene as the reference compound.[32] Holloway et al. report a value of k(OH + AAL) = (4.60 ± 0.19) × 10^{-11} cm^3 $molecule^{-1}$ s^{-1} at T = 298 ± 2 K in 100−300 Torr helium using a pulsed laser photolysis/laser-induced fluorescence technique with generation of OH radical by ultraviolet photolysis (λ = 248 nm) of 2,4-pentanedione.[33] Orlando et al. measured a value of k(OH + AAL) = (4.5 ± 0.6) × 10^{-11} cm^3 $molecule^{-1}$ s^{-1} at T = 298 K at 700 Torr of synthetic air using a relative rate method with propene as the reference compound.[34] Upadhyaya et al. report a value of k(OH + AAL) = (3.7 ± 0.5) × 10^{-11} cm^3 $molecule^{-1}$ s^{-1} at an unspecified "room temperature" in 10−20 Torr argon using a pulsed laser photolysis/laser-induced fluorescence technique with generation of OH radical by ultraviolet photolysis (λ = 193 nm) of the allyl alcohol.[35] Le Person et al. investigated this reaction using an absolute method and a relative method and report an average value of k(OH + AAL) = (5.0 ± 0.5) × 10^{-11} cm^3 $molecule^{-1}$ s^{-1} at T = 298 K.[44]

Our measured value of k(OH + AAL) at T = 298 K is (6.74 ± 1.35) × 10^{-11} cm^3 $molecule^{-1}$ s^{-1} and is in agreement with

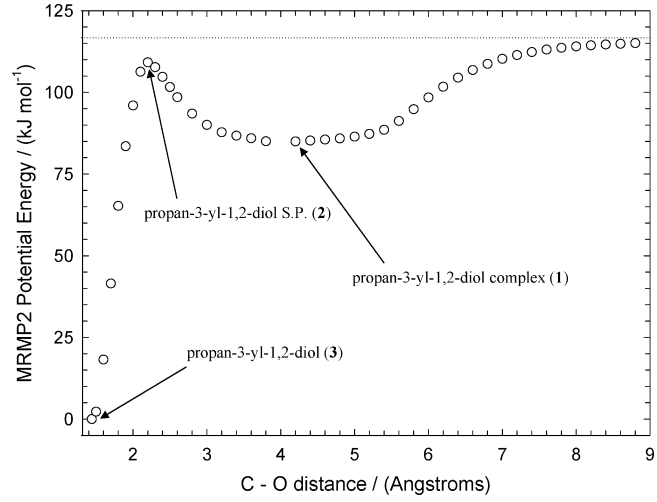

Figure 10. MRMP2 potential energy scan, not including zero-point vibrational energy, for addition of OH radical to AAL to form propan-3-yl-1,2-diol. A hydrogen-bonded complex is formed at the reaction entrance channel in the range of 3−5.5 Å; a saddle point (S.P.) occurs near 2 Å. The energy of the reaction asymptote is indicated by the dotted line.

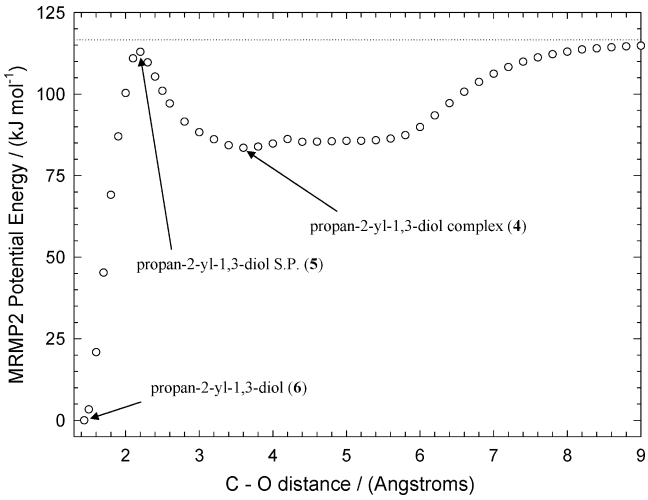

Figure 11. MRMP2 potential energy scan, not including zero-point vibrational energy, for addition of OH radical to AAL to form propan-2-yl-1,3-diol. A hydrogen-bonded complex is formed at the reaction entrance channel in the range of 3−6 Å; a saddle point (S.P.) occurs near 2 Å. The energy of the reaction asymptote is indicated by the dotted line.

that of Papagni et al. [$(5.46 \pm 0.35) \times 10^{-11}$ cm^3 molecule^{-1} s^{-1} at $T = 296$ K][32] within the experimental uncertainties. The experimental method used in the present work is very similar to the method used by Papagni et al., so it is not surprising that our value is in best agreement with theirs. Our value is in agreement with the averaged result reported by Le Person et al. [$(5.0 \pm 0.5) \times 10^{-11}$ cm^3 molecule^{-1} s^{-1} at $T = 298$ K].[44] Our value is slightly higher than that reported by Halloway et al. [$(4.60 \pm 0.19) \times 10^{-11}$ cm^3 molecule^{-1} s^{-1} at $T = 298$ K][33] and Orlando et al. [$(4.5 \pm 0.6) \times 10^{-11}$ cm^3 molecule^{-1} s^{-1} at $T = 298$ K].[34] Our value is significantly higher than that reported by Upadhyaya et al. [$(3.7 \pm 0.5) \times 10^{-11}$ cm^3 molecule^{-1} s^{-1}]. Because Upadhyaya et al. worked at reduced pressure (10−20 Torr), it is possible that the rate constant that they measured was in the falloff regime under their experimental conditions, as they note. This could explain why the value of k(OH + AAL) as measured by Upadhyaya et al. is the lowest in the data set. Gordon and Mulac[42] report a value of k(OH + AAL) = $(2.59 \pm 0.33) \times 10^{-11}$ cm^3 molecule^{-1} s^{-1} at $T = 440$ K using an absolute measurement technique. Extrapolation of the present data to $T = 440$ K predicts a rate constant of 2.05×10^{-11} cm^3 molecule^{-1} s^{-1}.

The results of the ab initio calculations at the MRMP2 level indicate that formation of propan-3-yl-1,2-diol (a primary carbon radical) from addition of OH radical to the π bond of AAL is slightly more exothermic (∼3.5 kJ mol^{-1}, Table 4) than formation of propan-2-yl-1,3-diol (a secondary carbon radical). This result is surprising given that the general trend for thermodynamic stability of organic radicals is tertiary > secondary > primary. Both of the product radicals are stabilized by an intramolecular hydrogen bond (Figure 12). The hydrogen bonding distance in these two radicals is nearly the same (∼2.4 Å). It is interesting to note that the saddle point for formation of propan-3-yl-1,2-diol is lower, by about 4.2 kJ mol^{-1}, than the corresponding saddle point for formation of propan-2-yl-1,3-diol. Therefore, it is expected that the predominant addition pathway for OH + AAL would be formation of propan-3-yl-1,2-diol, the primary carbon radical product. Upadhyaya et al. report results of ab initio calculations for optimized geometries of AAL + OH reactants and the propan-2-yl-1,3-diol and propan-3-yl-1,2-diol products at the HF/6-311G(d,p) level of theory. Single-point calculations were conducted at the QCISD(T) level using the same basis set. They found that formation of propan-2-yl-1,3-diol is exothermic by −105 kJ mol^{-1}; formation of propan-3-yl-1,2-diol is exothermic by −118 kJ mol^{-1}. They found that the primary carbon radical product is more stable than the secondary carbon radical product by ∼13 kJ mol^{-1}. Upadhyaya et al. do not report on prereaction hydrogen-bonded complexes or saddle points occurring on the reaction pathways.

The MCSCF calculations of our study indicate that hydrogen-bonded complexes form in the reactant entrance channels for addition of OH to the π bond of AAL; these complexes then rearrange through first-order saddle points to the indicated diol products. The minimum energy paths, structures, and energies of the complexes, saddle points, and diol products are given in Figures 10−12 and Table 4. The computational results show that addition of OH to AAL is not a simple elementary reaction, as one might suppose. Instead, the OH radical hydrogen bonds to the oxygen atom of AAL, forming complexes in the entrance channels that are stabilized by 25−33 kJ mol^{-1}. These complexes can then rearrange through saddle points that are +0.6 to +4.9 kJ mol^{-1} higher in energy than separated reactants, at the MRMP2 level.

A third reaction channel is available for AAL + OH: transfer of a hydrogen atom from the CH_2 group of AAL to OH to make prop-2-en-1-yl-1-ol radical and water (pathway 4c). The computed barrier for this transfer is −13.7 kJ mol^{-1}. The structure of the saddle point (**7**) is shown in Figure 12. That the saddle point has a negative relative energy implies that formation of a hydrogen bonded complex in this reaction entrance channel precedes formation of species **7**. We have not conducted a search for such a complex. We note that Papagni et al.[32] and Orlando et al.[34] measured acrolein formation yields of 5.5 ± 0.7% and 5 ± 2%, respectively, from the OH + allyl alcohol reaction, and this acrolein formation corresponds to the fraction of the overall OH + allyl alcohol reaction proceeding by H-atom abstraction from the CH_2OH group.

The measured temperature dependence for AAL + OH is strongly negative, with a factor of −1100 K occurring as the value of E_a/k_B in the exponential term of the Arrhenius expression. The observed negative temperature dependence for this reaction is expected. For comparison, the OH + ethene reaction has a value of −438 K for E_a/k_B, and OH reactions with other small alkenes containing only carbon and hydrogen have an E_a/k_B in the range of −450 to −550 K.[28] The implication is that the presence of the OH group in AAL makes the temperature dependence of the total rate constant more negative, as compared to hydrocarbon alkenes. The OH group in AAL serves as a hydrogen bond acceptor in the OH +AAL reaction and contributes to formation of hydrogen-bonded prereaction complexes, which is exhibited as a strongly negative temperature dependence in the total rate constant. This phenomenon is probably more general. For example, Cometto et al.[43] obtained temperature dependencies for the reactions of OH radicals with a series of C_4 and C_5 unsaturated alcohols, with the values of E_a/k_B ranging from −652 to −836 K, reasonably close to that measured in the present work for allyl alcohol and somewhat more negative than observed for the mentioned OH + alkene reactions.

We have also measured the rate constant for reaction of AAL-d_6 (fully deuterated AAL) with the OH radical. At $T = 298$ K, our measured value is $(5.1 \pm 0.2) \times 10^{-11}$ cm^3 molecule^{-1} s^{-1}. From our Arrhenius expression for AAL + OH, we find that $k = 6.7 \times 10^{-11}$ cm^3 molecule^{-1} s^{-1}. The kinetic isotope effect

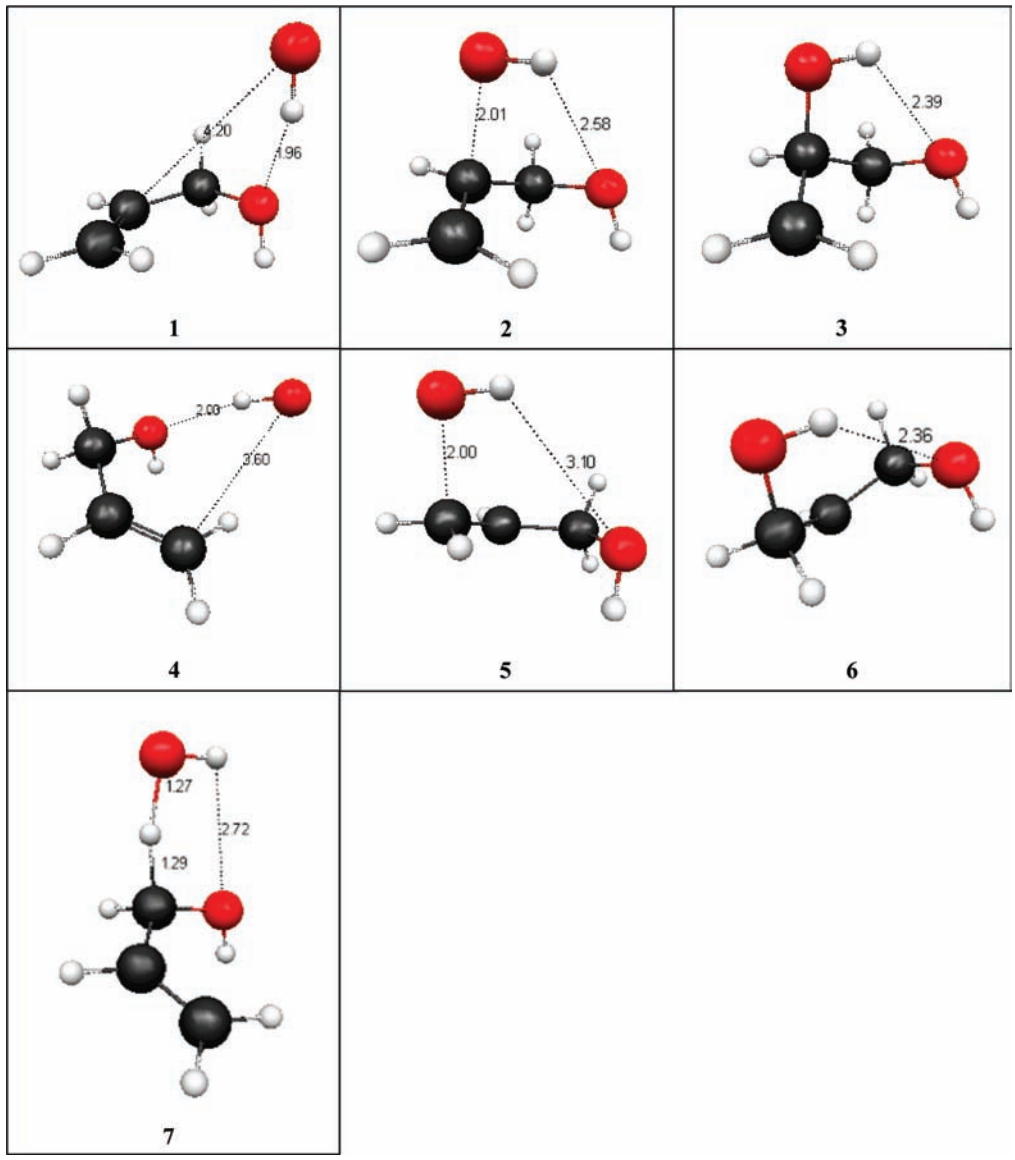

Figure 12. Pictorial representations of stationary points occurring along the minimum energy pathways for reaction of the OH radical with allyl alcohol, optimized at the (3,3)-MCSCF/6-311G(d,p) level of theory. Key interatomic distances (Å) are labeled. Numerical assignments correspond to structure names in Table 4.

TABLE 4: Relative Energies (kJ mol^{-1}) of Stationary Points for OH Radical Reaction with AAL

species	MCSCF	MRMP2
propan-3-yl-1,2-diol prereaction complex (**1**)	−19.69	−24.90
propan-3-yl-1,2-diol saddle point (**2**)	+44.98	+0.593
propan-3-yl-1,2-diol product (**3**)	−42.35	−99.77
propan-2-yl-1,3-diol prereaction complex (**4**)	−26.50	−33.08
propan-2-yl-1,3-diol saddle point (**5**)	+60.94	+4.870
propan-2-yl-1,3-diol product (**6**)	−37.36	−96.19
AAL/OH abstraction saddle point (**7**)	+78.09	−13.70
OH + AAL asymptote	0.0	0.0

is $k(\text{AAL})/k(\text{AAL-}d_6) = 1.3$. Because the value of the experimental rate constant is lowered only moderately upon deuteration of AAL, we conclude that most of the reaction proceeds by addition of the OH radical to AAL, with a small amount likely due to H-atom transfer (channel 4c).

The kinetics of the reaction of AAL with NO_3 radical have been studied previously by Hallquist et al.[36] They directly measured the rate constant for this reaction in the range $T = 273-363$ K using a fast flow reactor with chemical generation of NO_3 from the reaction of F + HNO_3 and laser diode detection of the NO_3 radical. In addition, they used a relative rate technique with propene as the reference to measure the rate constant at $T = 294$ K. At this temperature, their measured values of the rate constant for AAL + NO_3 are $(1.3 \pm 0.2) \times 10^{-14}$ cm^3 $molecule^{-1}$ s^{-1} from the fast flow reactor and $(1.6 \pm 0.4) \times 10^{-14}$ cm^3 $molecule^{-1}$ s^{-1} from the relative rate experiment. Our measured value of the rate constant for AAL + NO_3 is $(7.7 \pm 0.2) \times 10^{-15}$ cm^3 $molecule^{-1}$ s^{-1} and is a factor of ~2 less than those values of Hallquist et al. The primary difference in the way we carried out our relative rate experiment as compared to the Hallquist experiment is that we generated NO_3 radicals by thermal decomposition of N_2O_5, whereas Hallquist formed NO_3 radical in situ by reaction of NO_2 with O_3. It seems to us that the in situ route to NO_3 is less preferable, since there is a possibility of loss of some of the AAL to O_3 if the NO_2 + O_3 reaction is not taken to completion. Loss of AAL to O_3 in the NO_3 relative rate constant experiment would lead to an erroneously high value of $k(NO_3 + \text{AAL})$. Regarding the absolute rate constant measurements, it is not clear to us that Hallquist et al. worked under conditions such that all of the F atoms in the F + HNO_3 reaction were consumed

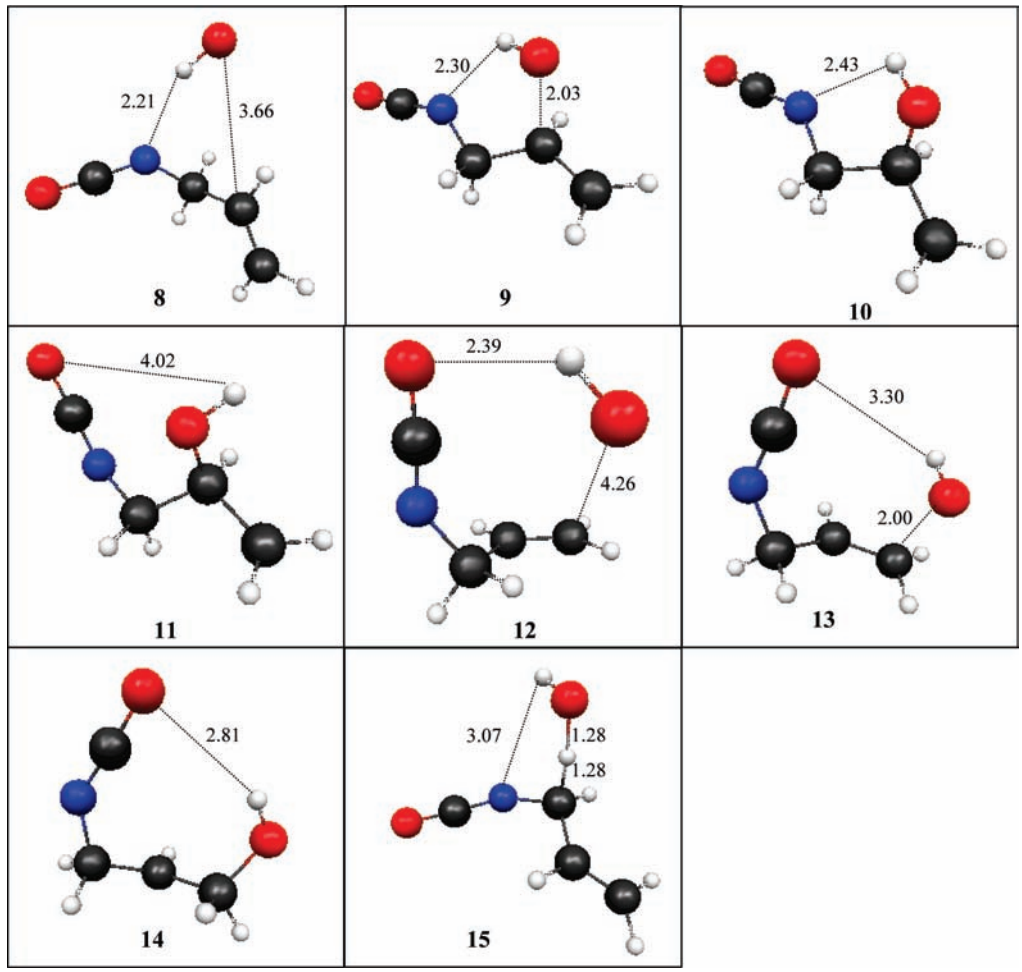

Figure 13. Pictorial representations of stationary points occurring along the minimum energy pathways for reaction of OH radical with allyl isocyanate, optimized at the (3,3)-MCSCF/6-311G(d,p) level of theory. Key interatomic distances (Å) are labeled. Numerical assignments correspond to structure names in Table 5.

by HNO_3 and that no significant amount of F was undergoing reaction with AAL. Because of these considerations, there is some doubt as to the accuracy of the Hallquist data.

We have measured the rate constant for reaction of AAL-d_6 with NO_3 radical. We find a value of $k(NO_3 + \text{AAL-}d_6) = (7.6 \pm 0.2) \times 10^{-15}$ cm^3 molecule^{-1} s^{-1} at $T = 298$ K. Because there is no significant difference in the measured rate constants for reaction of NO_3 with AAL or AAL-d_6, we postulate that the NO_3 + AAL reaction mechanism is addition of NO_3 to the π bond of AAL.

We have measured the rate constant for reaction of AAL with O_3 at $T = 296$ K, and we find a value of $k(\text{AAL} + O_3) = (1.63 \pm 0.03) \times 10^{-17}$ cm^3 molecule^{-1} s^{-1}. This compares well with a previously measured absolute value of $k(\text{AAL} + O_3) = (1.44 \pm 0.20) \times 10^{-17}$ cm^3 molecule^{-1} s^{-1}, as measured by Grosjean et al.[37]We have also measured the rate constant for reaction of AAL-d_6 with O_3, and the value is $k(\text{AAL-}d_6 + O_3) = (1.84 \pm 0.03) \times 10^{-17}$ cm^3 molecule^{-1} s^{-1}. This value is not significantly different from that measured for $k(\text{AAL}+O_3)$, as expected.

We have carried out relative rate constant measurements for the reaction of the OH radical with AIC (allyl isocyanate). This is the first report in the literature of the rate constant for this reaction. The experimentally determined Arrhenius expression for this radical/molecule reaction is: $k(\text{OH} + \text{AIC}) = 1.94 \times 10^{-14} \times \exp[(2207 \pm 158)/T]$ cm^3 molecule^{-1} s^{-1}. The value of E_a/k_B is -2207 K and is a factor of 2 more negative than E_a/k_B for the OH + AAL reaction.

TABLE 5: Relative Energies (kJ mol^{-1}) of Stationary Points for OH Radical Reaction with AIC

species	MCSCF	MRMP2
propan-3-yl-1-isocyano-2-ol prereaction complex (**8**)	−10.44	−17.81
propan-3-yl-1-isocyano-2-ol saddle point (**9**)	+66.58	−4.02
propan-3-yl-1-isocyano-2-ol product A (**10**)	−46.71	−102.25
propan-3-yl-1-isocyano-2-ol product B (**11**)	−48.64	−108.20
propan-2-yl-1-isocyano-3-ol prereaction complex (**12**)	−12.09	−16.47
propan-2-yl-1-isocyano-3-ol saddle point (**13**)	+60.59	−14.03
propan-2-yl-1-isocyano-3-ol product (**14**)	−28.26	−89.59
AIC/OH abstraction saddle point (**15**)	+81.39	−16.02
OH + AIC asymptote	0.0	0.0

The mechanism for the OH + AIC reaction has been studied quantum mechanically at the MRMP2/6-311G(d,p) level of theory. Referring to Figure 13, Table 5, and reactions 5a−c, we find three reaction channels. In reaction channel 5a, OH radical forms the hydrogen bonded prereaction complex **8** with AIC in the reaction entrance. Complex **8** is stabilized by −17.8 kJ mol^{-1} with respect to separated reactants. Complex **8** contains an intramolecular hydrogen bond between the OH radical and the N atom of AIC. Complex **8** may rearrange through first-order saddle point **9**, which is −4.0 kJ mol^{-1} lower in energy than separated reactants. Saddle point **9** conserves the intramolecular hydrogen bond of complex **8**. Saddle point **9** may then form product **10** at −102 kJ mol^{-1} in energy. Product **10** can interconvert with product **11** at −108 kJ mol^{-1} in energy. It is interesting to note that product **11** does not conserve the

intramolecular hydrogen bond, yet it is lower in energy than product **10**. Products **10** and **11** are primary carbon-centered radicals.

The second reaction channel for OH + AIC is designated as channel 5b. In the entrance to channel 5b, the OH radical forms hydrogen bonded prereaction complex **12** with AIC. Complex **12** is stabilized by −16.5 kJ mol^{-1} with respect to separated reactants. Complex **12** contains an intramolecular hydrogen bond between the OH radical and the O atom of AIC. Complex **12** may rearrange through first-order saddle point **13**, which is −14.0 kJ mol^{-1} lower in energy than separated reactants. The distance between the H atom of the OH moiety and the O atom of the AIC moiety in complex **13** is 3.30 Å. This distance is probably too long to be considered a hydrogen bond. Saddle point **13** then forms product **14**, with an intramolecular hydrogen bond distance of 2.8 Å. Product **14** is −89.6 kJ mol^{-1} below the energy of separated reactants. Product **14** is a secondary carbon-centered radical. It is interesting to note that formation of products **10** and **11**, both of which are primary carbon-centered radicals, is significantly more exoergic (12−18 kJ mol^{-1}) than formation of product **14**. This phenomenon was also observed for reaction of OH with AAL.

A third reaction channel for OH + AIC is designated as channel 5c. Channel 5c involves transfer of a hydrogen atom from the CH_2 group of AIC to the OH radical, forming water and the corresponding radical. We have located the saddle point for this reaction channel. It is designated as species **15** in Figure 13. Saddle point **15** is calculated to be −16.0 kJ mol^{-1} below the energy of separated reactants. That saddle point **15** is submerged implies that there is a prereaction complex that precedes it in the reaction entrance channel. We have not attempted a search for such a complex.

We have noted that the experimentally observed temperature dependence for the OH + AIC reaction is about a factor of 2 more negative than the OH + AAL reaction. This observation is in line with the calculated energies of the saddle points that occur in each of the three channels for both reactions. In each case, the saddle points of channels 5a, b, and c lie lower in energy than the saddle points in the corresponding channels of 4a, b, and c. The implication is that the calculations are correct in determining the relative energies of the saddle points in each of the reaction channels, although these energies are not expected to be chemically accurate (i.e., accurate to within ±4 kJ mol^{-1} of the true values).

We have measured the rate constants for reactions of the NO_3 radical and O_3 with AIC. These are the first reported rate constants for these reactions. Near ambient room temperature, the rate constant for NO_3 + AIC reaction was found to be (9.4 ± 0.6) × 10^{-16} cm^3 $molecule^{-1}$ s^{-1}; the rate constant for reaction of O_3 + AIC was found to be (5.54 ± 0.45) × 10^{-15} cm^3 $molecule^{-1}$ s^{-1}. Each of these rate constants is lower than the corresponding rate constants for reactions of AAL.

Atmospheric Implications. The tropospheric lifetimes of AAL and AIC can be estimated from the measured rate constants for reactions with OH, NO_3, and O_3 and from the average tropospheric concentrations of OH, NO_3, and O_3 of 9.4 × 10^5 (24 h global average[38]), 5.0 × 10^8 (12 h nighttime average[28,39]), and 7.0 × 10^{11} (24 h average[28,40]) molecules cm^{-3}, respectively. For AAL, the OH, NO_3, and O_3 lifetimes are 4.4, 72, and 24 h, respectively. The dominant chemical loss pathway for AAL in the troposphere is predicted to be reaction with OH radical. This is not surprising. However, significant losses to reaction with ozone and NO_3 radical are expected. For AIC, the OH, NO_3, and O_3 lifetimes are 9.3 h, 25 days, and 72 h, respectively. Most of the chemical loss of AIC in the troposphere is expected to occur by reaction with the OH radical and a small loss due to reaction with ozone. Reaction of AIC with the NO_3 radical is not expected to be important in the troposphere.

Acknowledgment. Financial support of this work was provided by an Internal Research and Development grant from Midwest Research Institute. The authors are grateful for this support. We thank Mr. Pete Deardorff and Dr. Bruce Diel for providing samples of methyl nitrite and dinitrogen pentoxide.

Supporting Information Available: A table containing absolute electronic energies and zero point vibrational energies for species **1**−**15** is available as Supporting Information (Table S1). This material is available free of charge via the Internet at http://pubs.acs.org.

References and Notes

(1) Finlayson-Pitts, B. J.; Pitts, J. N., Jr. *Chemistry of the Upper and Lower Atmosphere*; Academic Press: San Diego, 2000.
(2) Grosjean, E.; Grosjean, D. *J. Atomos. Chem.* **1999**, *32*, 205.
(3) Hoffman, T.; Odum, J. R.; Bowman, F.; Collins, D.; Klockow, D.; Flagan, R. C.; Seinfeld, J. H. *J. Atmos. Chem.* **1997**, *26*, 189.
(4) Mellouki, A.; LeBras, G.; Sidebottom, H. *Chem. Rev.* **2003**, *103*, 5077.
(5) Kanakidou, M.; Seinfeld, J. H.; Pandis, S. N.; Barnes, I.; Dentener, F. J.; Facchini, M. C.; van Dingenen, R.; Ervens, B.; Nenes, A.; Nielsen, C. J.; Swietlicki, E.; Putaud, J. P.; Balkanski, Y.; Fuzzi, S.; Horth, J.; Moortgat, G. K.; Winterhalter, R.; Myhre, C. E. L.; Tsigaridis, K.; Vignati, E.; Stephanou, E. G.; Wilson, J. *Atmos. Chem. Phys.* **2005**, *5*, 1053.
(6) Hansen, J. C.; Francisco, J. S. *Chem. Phys. Chem.* **2002**, *3*, 833.
(7) Parker, J. K.; Espada-Jallad, C.; Parker, C. L.; Witt, J. D. *Int. J. Chem. Kinet.* **2009**, *41*, 187.
(8) Schmidt, M. W.; Baldridge, K. K.; Boatz, J. A.; Elbert, S. T.; Gordon, M. S.; Jensen, J. H.; Koseki, S.; Matsunaga, N.; Nguyen, K. A.; Su, S. J.; Windus, T. L.; Dupuis, M.; Montgomery, J. A. *J. Comput. Chem.* **1993**, *14*, 1347.
(9) Schmidt, M. W.; Gordon, M. S. *Annu. Rev. Phys. Chem.* **1998**, *49*, 233.
(10) Pople, J. A.; Nesbet, R. K. *J. Chem. Phys.* **1954**, *22*, 571.
(11) McWeeny, R.; Dierksen, G. *J. Chem. Phys.* **1968**, *49*, 4852.
(12) Ditchfield, R.; Hehre, W. J.; Pople, J. A. *J. Chem. Phys.* **1971**, *54*, 724.
(13) Hehre, W. J.; Ditchfield, R.; Pople, J. A. *J. Chem. Phys.* **1972**, *56*, 2257.
(14) Hariharan, P. C.; Pople, J. A. *Mol. Phys.* **1974**, *27*, 209.
(15) Gordon, M. S. *Chem. Phys. Lett.* **1980**, *76*, 163.
(16) Hariharan, P. C.; Pople, J. A. *Theor. Chim. Acta* **1973**, *28*, 213.
(17) Blaudeau, J.-P.; McGrath, M. P.; Curtiss, L. A.; Radom, L. *J. Chem. Phys.* **1977**, *107*, 5016.
(18) Francl, M. M.; Pietro, W. J.; Hehre, W. J.; Binkley, J. S.; DeFrees, D. J.; Pople, J. A.; Gordon, M. S. *J. Chem. Phys.* **1982**, *77*, 3654.
(19) Binning, R. C., Jr.; Curtiss, L. A. *J. Comput. Chem.* **1990**, *11*, 1206.
(20) Rassolov, V. A.; Pople, J. A.; Ratner, M. A.; Windus, T. L. *J. Chem. Phys.* **1998**, *109*, 1223.
(21) Rassolov, V. A.; Ratner, M. A.; Pople, J. A.; Redfern, P. C.; Curtiss, L. A. *J. Comput. Chem.* **2001**, *22*, 976.
(22) McLean, A. D.; Chandler, G. S. *J. Chem. Phys.* **1980**, *72*, 5639.
(23) Krishnan, R.; Binkley, J. S.; Seeger, R.; Pople, J. A. *J. Chem. Phys.* **1980**, *72*, 650.
(24) Clark, T.; Chandrasekhar, J.; Spitznagel, G. W.; Schleyer, P. v. R. *J. Comput. Chem.* **1983**, *4*, 294.
(25) Frisch, M. J.; Pople, J. A.; Binkley, J. S. *J. Chem. Phys.* **1984**, *80*, 3265.
(26) Hirao, K. *Chem. Phys. Lett.* **1992**, *190*, 374.
(27) Hirao, K. *Chem. Phys. Lett.* **1992**, *196*, 397.
(28) Atkinson, R.; Arey, J. *Chem. Rev.* **2003**, *103*, 4605.
(29) Geiger, H.; Barnes, I.; Becker, K. H.; Bohn, B.; Brauers, T.; Donner, B.; Dorn, H.-P.; Elend, M.; Dinis, C. M. F.; Grossmann, D.; Hass, H.; Hein, H.; Hoffmann, A.; Hoppe, L.; Hülsemann, F.; Kley, D.; Klotz, B.; Libuda, H. G.; Maurer, T.; Mihelcic, D.; Moortgat, G. K.; Olariu, R.; Neeb, P.; Poppe, D.; Ruppert, L.; Sauer, C. G.; Shestakov, O.; Somnitz, H.; Stockwell, W. R.; Thüner, L. P.; Wahner, A.; Wiesen, P.; Zabel, F.; Zellner, R.; Zetzsch, C. *J. Atmos. Chem.* **2002**, *42*, 323.
(30) Morris, E. D., Jr.; Niki, H. *J. Phys. Chem.* **1974**, *78*, 1337.
(31) Japar, S. M.; Niki, H. *J. Phys. Chem.* **1975**, *79*, 1629.
(32) Papagni, C.; Arey, J.; Atkinson, R. *Int. J. Chem. Kinet.* **2001**, *33*, 142.

(33) Holloway, A.-L.; Treacy, J.; Sidebottom, H.; Mellouki, A.; Daële, V.; Le Bras, G.; Barnes, I. *J. Photochem. Photobiol., A* **2005**, *176*, 183.
(34) Orlando, J. J.; Tyndall, G. S.; Ceazan, N. *J. Phys. Chem. A* **2001**, *105*, 3564.
(35) Upadhyaya, H. P.; Kumar, A.; Naik, P. D.; Sapre, A. V.; Mittal, J. P. *Chem. Phys. Lett.* **2001**, *349*, 279.
(36) Hallquist, M.; Langer, S.; Ljungström, E.; Wängberg, I. *Int. J. Chem. Kinet.* **1996**, *28*, 467.
(37) Grosjean, D.; Grosjean, E.; Williams, E. L., II. *Int. J. Chem. Kinet.* **1993**, *25*, 783.
(38) Prinn, R. G.; Huang, J.; Weiss, R. F.; Cunnold, D. M.; Fraser, P. J.; Simmons, P. G.; McCulloch, A.; Harth, C.; Salameh, P.; O'Doherty, S.; Wang, R. H. J.; Porter, L.; Miller, B. R. *Science* **2001**, *292*, 1882.
(39) Platt, U.; Heintz, F. *Isr. J. Chem.* **1994**, *34*, 289.
(40) Atkinson, R. *J. Phys. Chem. Ref. Data* **1991**, 459.
(41) Aschmann, S. M.; Long, W. D.; Atkinson, R. *J. Phys. Chem. A* **2006**, *110*, 7393.
(42) Gordon, S.; Mulac, W. A. *Int. J. Chem. Kinet.*, Symp. 1, *289*, **1975**.
(43) Cometto, P. M.; Dalmasso, P. R.; Taccone, R. A.; Lane, S. I.; Oussar, F.; Daele, V.; Mellouki, A.; Le Bras, G. *J. Phys. Chem. A* **2008**, *112*, 4444.
(44) Le Person, A.; Solignac, G.; Oussar, F.; Daele, V.; Mellouki, A.; Winterhalter, R.; Moortgat, G. K. *Phys. Chem. Chem. Phys.* **2009**; DOI 10.1039/b905776e.

JP9055939